The oligomeric state and stability of the mannitol transporter, EnzymeII^{mtl}, from *Escherichia coli*: A fluorescence correlation spectroscopy study

GERTJAN VELDHUIS,[1] MARK HINK,[2] VICTOR KRASNIKOV,[1]
GEERT VAN DEN BOGAART,[1] JEROEN HOEBOER,[1] ANTONIE J.W.G. VISSER,[2]
JAAP BROOS,[1] AND BERT POOLMAN[1]

[1]Department of Biochemistry and Biophysical Chemistry, Groningen Biomolecular Science and Biotechnology Institute & Materials Science Centre^{plus}, University of Groningen, 9747 AG Groningen, The Netherlands
[2]MicroSpectroscopy Centre, Wageningen University, 6700 ET Wageningen, The Netherlands

(RECEIVED January 25, 2006; FINAL REVISION April 11, 2006; ACCEPTED April 14, 2006)

Abstract

Numerous membrane proteins function as oligomers both at the structural and functional levels. The mannitol transporter from *Escherichia coli*, EnzymeII^{mtl}, is a member of the phosphoenolpyruvate-dependent phosphotransferase system. During the transport cycle, mannitol is phosphorylated and released into the cytoplasm as mannitol-1-phosphate. Several studies have shown that EII^{mtl} functions as an oligomeric species. However, the oligomerization number and stability of the oligomeric complex during different steps of the catalytic cycle, e.g., substrate binding and/or phosphorylation of the carrier, is still under discussion. In this paper, we have addressed the oligomeric state and stability of EII^{mtl} using fluorescence correlation spectroscopy. A functional double-cysteine mutant was site-specifically labeled with either Alexa Fluor 488 or Alexa Fluor 633. The subunit exchange of these two batches of proteins was followed in time during different steps of the catalytic cycle. The most important conclusions are that (1) in a detergent-solubilized state, EII^{mtl} is functional as a very stable dimer; (2) the stability of the complex can be manipulated by changing the intermicellar attractive forces between PEG-based detergent micelles; (3) substrate binding destabilizes the complex whereas phosphorylation increases the stability; and (4) substrate binding to the phosphorylated species partly antagonizes the stabilizing effect.

Keywords: EnzymeII; mannitol transporter; fluorescence correlation spectroscopy; oligomeric state; oligomeric stability

Many membrane proteins reside as oligomeric species in the lipid bilayer. However, it is often not clear if and how oligomeric substates participate in the catalytic cycle, as the oligomeric state can be a dynamic parameter. Some membrane proteins reside in the membrane as monomers and function as such, e.g., the sugar-phosphate anti-porter UhpT and the lactose carrier LacY (Ambudkar et al. 1990; Sahin-Toth et al. 1994), whereas others may function as

Reprint requests to: Bert Poolman, Department of Biochemistry and Biophysical Chemistry, Groningen Biomolecular Science and Biotechnology Institute & Materials Science Centre^{plus}, University of Groningen, Nijenborgh 4, 9747 AG Groningen, The Netherlands; e-mail: b.poolman@rug.nl; fax: +31-50-3634165.

Abbreviations: AF, Alexa Fluor; $C_{10}E_5$, decyl pentaethylene glycol ether; decylPEG, decylpoly(ethylene glycol)300; DTT, dithiothreitol; EI, Enzyme I from *Escherichia coli*; FCCS, fluorescence cross-correlation spectroscopy; FCS, fluorescence correlation spectroscopy; HPr, heat-stable protein from *Escherichia coli*; Mtl, mannitol; PEP, phosphoenolpyruvate; PTS, PEP-dependent phosphotransferase system; EII^{mtl}, wild-type EnzymeII^{mtl} from *Escherichia coli*; EII-SSCS, EII^{mtl} where three of the four native cysteines in wild-type EII^{mtl} (Cys110, Cys320, Cys571) have been replaced by serines, but the catalytically important Cys384 is intact; EII-R636C, double-cysteine mutant based on EII-SSCS with an additional cysteine replacing residue Arg636; EII-AF488/633, EII-R636C alkylated with Alexa fluorophores 488/633, respectively, at Cys636.

Article published online ahead of print. Article and publication date are at http://www.proteinscience.org/cgi/doi/10.1110/ps.062113906.

dimers or higher state oligomers, e.g., the multidrug transporter EmrE (Ubarretxena-Belandia and Tate 2004). The lactose transporter from *Streptococcus thermophillus* (LacS) is structurally a dimer both in the membrane and in a detergent-solubilized state (Friesen et al. 2000). While a single subunit harbors the full translocation path and is able to perform exchange transport, functional interactions between two subunits can be observed for both exchange and proton-motive-force-driven uptake of lactose (Veenhoff et al. 2001; Geertsma et al. 2005). For the glucose transporter GLUT1 from erythrocytes, the oligomeric state of the protein is also a determining factor for activity (Hebert and Carruthers 1992). Oligomeric state-dependent functioning of membrane proteins has been suggested for more proteins, such as the tetracycline transporter TetA, the Na^+/H^+ anti-porter NhaA from *Escherichia coli*, and the ion exchanger Band 3 in erythrocytes (Casey and Reithmeier 1991; Yin et al. 2000; Gerchman et al. 2001). Experimental data regarding the quaternary structure of membrane proteins in the detergent-solubilized and the (native) membrane-embedded state are difficult to obtain due to the complexity of the system. In the last decade, fluorescence correlation spectroscopy (FCS) has been developed to address the oligomeric state of (water-soluble) proteins under in vitro and in vivo conditions. Recently, the oligomeric state of a membrane protein (the somatic embryogenesis receptor kinase 1 of *Arabidopsis thaliana*, AtSERK1) has been investigated by confocal microscopy (Hink 2002). We have adopted the FCS technique to investigate the oligomeric state and stability of the mannitol transporter, EnzymeII^{mtl} (EII^{mtl}), from *E. coli* in detergent solution during different steps of its catalytic cycle.

In *E. coli*, EII^{mtl} is responsible for the uptake of the sugar mannitol. EII^{mtl} is part of the PEP-dependent phosphotransferase system (PTS); members of this class of transport proteins are group translocators that chemically modify their substrate during transport (for review, see Robillard and Broos 1999). EII^{mtl} consists of a single polypeptide chain of 637 amino acids, comprising three domains: a membrane-embedded IIC^{mtl}-domain, harboring the mannitol translocation path, and two cytosolic domains (IIB^{mtl} and IIA^{mtl}) responsible for phosphoryl group transfer reactions. The phosphoryl group originates from PEP and is transferred to the IIA^{mtl}-domain via two soluble energy-coupling proteins, EnzymeI and HPr. P-IIA^{mtl} then donates the phosphate to IIB^{mtl}. Mannitol, bound at the IIC^{mtl}-domain, becomes phosphorylated and is subsequently released into the cytoplasm as mannitol-1-phosphate.

The oligomeric structure of EII^{mtl} has been subjected to several investigations (Saier 1980; Leonard and Saier 1983; Roossien and Robillard 1984; Roossien et al. 1984, 1986; Stephan and Jacobson 1986; Pas et al. 1987; Robillard and Blaauw 1987; Khandekar and Jacobson 1989; Lolkema and Robillard 1990). From these studies it has been concluded that the associated state of EII^{mtl}, most likely a dimeric species, is responsible for high-affinity mannitol binding and mannitol phosphorylation. The crucial contacts within the oligomer have been attributed to IIC/IIC-domain interactions. The evidence arose from several biochemical approaches: (1) gel-filtration experiments (Lolkema et al. 1993a), (2) in vivo functional complementation of inactive proteins with mutations at different sites (White and Jacobson 1990; Briggs et al. 1992; Weng et al. 1992; Weng and Jacobson 1993; Boer et al. 1996; Saraceni-Richards and Jacobson 1997), and (3) in vitro complementation of pairs of inactive mutants (Stephan et al. 1989; White and Jacobson 1990; Van Weeghel et al. 1991a,b; Briggs et al. 1992; Boer et al. 1994, 1996; Broos et al. 1998).

Although EII^{mtl} is predominantly in the associated state both in the membrane and in the detergent-solubilized state, the influence of substrate binding and/or protein phosphorylation on the oligomeric stability of EII^{mtl} is still unclear. In this article, we address the dynamics of the oligomeric state of EII^{mtl} in the substrate-bound conformation and in the phosphorylated state, using fluorescence (cross)correlation spectroscopy (FCS and FCCS) (for reviews, see Eigen and Rigler 1994; Schwille et al. 1997; Haustein and Schwille 2003, 2004; Gösch and Rigler 2005).

Results

Catalytic properties of the mutants

Mutant EII-R636C bound mannitol with high affinity both in native membranes and decylPEG-solubilized ISO membrane vesicles, yielding K_D-values of 57 and 78 nM, respectively, comparable to wild-type and EII-SSCS (Van Montfort et al. 2001; Veldhuis et al. 2004, 2005a). The corresponding specific phosphorylation activities in both intact and detergent-solubilized membranes were 2600 min^{-1}, comparable to those of N-terminally his-tagged EII^{mtl} (Van Montfort et al. 2001; Veldhuis et al. 2005b). Purification of EII-R636C resulted in a specific phosphorylation activity of 580 min^{-1}, in line with previous observations (Van Montfort et al. 2001).

In order to specifically couple a fluorophore to Cys636, the active-site cysteine (Cys384) had to be protected from labeling by phosphorylation. Phospho-protection of Cys384 was achieved by incubation of the enzyme with PEP and the phosphoryl transfer proteins enzyme I and HPr (as described in Materials and Methods). The phospho-protection of Cys384 in EII-R636C was evaluated, using NEM as alkylating reagent in the absence or the presence of PEP. Following protection and 30 min of incubation with NEM, the specific phosphorylation activity was 570 min^{-1}, whereas without PEP the activity had dropped to <100 min^{-1}. Thus,

under these Cys384-protecting conditions, >95% of the activity was retained, and the method proved suitable for the specific labeling of Cys636 with fluorophores. The ~15% residual activity in the absence of phospho-protection probably reflects partial oxidation of Cys384. Oxidized Cys384 is also resistant to alkylation, and the oxidized cysteine is subsequently reduced by the DTT or β-mercaptoethanol present in the assay buffers (see also Veldhuis et al. 2005a).

Labeling of EII-R636C with Alexa fluorophores

Labeling of EII-R636C with Alexa fluorophores was carried out as described above for NEM. In Figure 1, the specific phosphorylation activities of EII-R636C are shown for each step of the phospho-protection protocol, using AF488 as alkylating reagent. Labeling of EII-R636C with AF488 resulted in a small decrease in the specific phosphorylation activity that was Alexa Fluor–specific, since it was not observed with NEM. The high residual activity confirms the effectiveness of the phospho-protection and demonstrates that labeling of Cys384 was minimal. Importantly, the alkylation of phospho-protected EII-R636C with the fluorophores resulted in a defined shift in the migration of the protein bands on SDS-PAGE (data not shown). Because the shift was not observed with the wild-type (phospho-protected Cys384) enzyme, we conclude that >90% of the label was positioned at Cys636 and that aspecific labeling was insignificant. The specific phosphorylation activities of EII-AF488 and EII-AF633 were similar. For both fluorophores, the labeling of EII-R636C at Cys636 was close to unity: 109% and 91%, respectively (the differences were within an error of ±10% of the used analysis method).

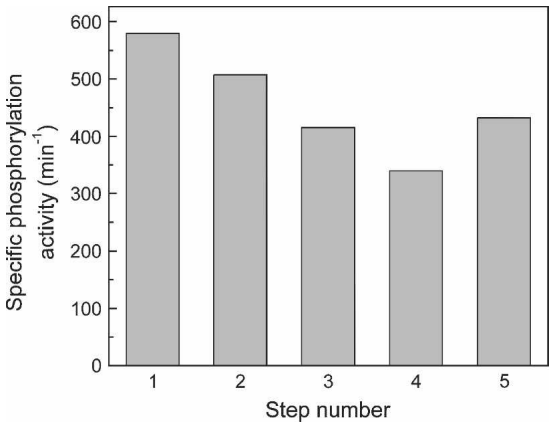

Figure 1. Specific phosphorylation activities of EII-R636C at the different steps of labeling with AF488 (see Materials and Methods for details of the protocol). The starting concentration EII-R636C in step 1 was 6.7 μM. The concentrations of EII-R636C in steps 2–4 were estimated on the basis of dilution of the sample in step 1 and small losses during desalting. The error in these specific phosphorylation activities is therefore 10%–20%. The concentration of protein and label of sample 5 was estimated on the basis of absorption spectroscopy (see Materials and Methods). The specific phosphorylation activities are in nM mannitol-1-P per minute per nM EII-R636C (min^{-1}). Description of the different steps: (1) starting material after reduction, (2) first desalting step, (3) sample after labeling with Alexa Fluor 488, (4) second desalting step, and (5) final fraction after elution from Q-Sepharose.

Fluorescence correlation spectroscopy

The oligomeric state of EII^{mtl} is difficult to extract from single-color FCS measurements, that is, on the basis of differences in diffusion times between monomers and dimers. A doubling of the mass (M) of a (spherical) particle results in an increase in the hydrodynamic radius (R_h) of only 26%, according to $R_h \propto \sqrt[3]{M}$. The Stokes-Einstein relationship predicts that the diffusion coefficient, D, is related to R_h of a particle according to $D = kT/6\pi\eta R_h$, where k is the Boltzmann constant; T, the temperature; and η, the viscosity of the medium. Therefore, if the mass of the particle doubles, the change in diffusion coefficient is relatively small. Furthermore, little is known about the amount of detergent that binds to different oligomeric species. It is therefore not possible to distinguish mono- and dimeric species on the basis of their individual diffusion times using single-color FCS (Meseth et al. 1999). FCCS is a technique that is not limited by the low resolving power in the diffusion times. In FCCS, particles labeled with two spectrally separated fluorescent dyes are simultaneously excited by two different lasers (Schwille et al. 1997). The two spectrally different fluorescent signals are split, which enables monitoring the fluorescence of the dyes individually. Photon bursts detected in both channels are cross-correlated. The cross-correlation function (namely, its amplitude) is determined by the product of the concentration of diffusing particles carrying both dyes and the effective observation volume. Therefore, FCCS can be used for monitoring association/dissociation kinetics and measuring binding equilibriums.

The two observation volumes of the two lasers will never overlap perfectly. Therefore, to correct for this spatial misalignment, the cross-correlation efficiency (a decrease in the magnitude of the cross-correlation amplitude as compared with that of an ideal system) must be evaluated. For this, autocorrelation curves of double-labeled DNA oligomers were recorded for both the green and red dyes as well as the cross-correlation signal (see Materials and Methods). The typical results are shown in Figure 2, and the fitting parameters are summarized in Table 1. The measured concentration of red-labeled DNA oligomers was higher than that of green-labeled DNA oligomers. Assuming that all green-labeled DNA was hybridized to a red-labeled DNA oligomer, the concentration

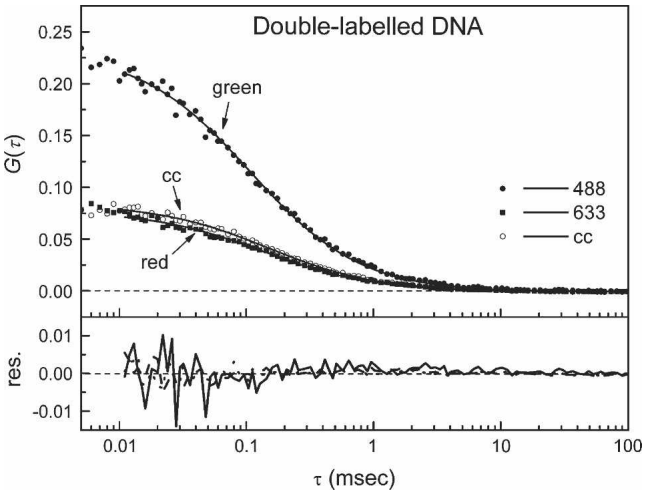

Figure 2. Autocorrelation curves of the double-labeled DNA. Shown are the autocorrelation curves of the AF488- (solid circle, solid line) and AF633- (solid square, dashed line) labeled oligomer and the cross-correlation curve (cc) (open circles, dotted line) to evaluate and calibrate the confocal setup. The curves were fitted using a one-species 3D-diffusion model (see residuals). Analysis showed that the cross-correlation efficiency was ~80%.

of double-stranded particles is equal to ~24 particles/μm^3. The presence of red-labeled, single-stranded DNA, which is half the molecular weight of double-stranded DNA, is likely the cause of a slight increase in the measured diffusion coefficient using 633 nm excitation as compared with 488 nm excitation (Table 1). In the case of an ideal spatial overlap of the green and red observation volumes, and considering the data in Table 1, the effective particle number for cross-correlation should be ~12 instead of the measured 15. For this, Equations 3 and 4 are used with $Q = 1$. Therefore, we estimate the cross-correlation efficiency of the setup to be ~80%. This value was used for correction of the measured $G_{g,r}(0)$ (Equation 6).

Subunit exchange as a function of the buffer system

Polyethyleneglycol (PEG)-based detergents (such as decylPEG and $C_{10}E_5$) in aqueous solutions show phase separation of detergent micelles above the so-called cloud point T_D (Zulauf 1991). Upon increasing the temperature, the hydration of the PEG chains is decreased, resulting in an increase in the attractive intermicellar forces and increasing aggregation of the micelles. Instead of heating the mixture, micelle aggregation at a fixed temperature can also be induced by adding strongly water-binding salts (e.g., sodium phosphate) or by adding a PEG-based detergent with a lower T_D (e.g., $C_{10}E_4$). This property of the detergents has been used to alter the hydrophobic forces of the subunit interactions in EII^{mtl}, and resulted in a decrease in the phosphorylation activity and increased rates of subunit exchange between two different inactive EII^{mtl} mutants (Broos et al. 1998). A similar strategy in combination with confocal microscopy was used here to investigate the oligomeric stability of EII^{mtl} by using mixtures of AF488- and AF633-labeled EII-R636C.

Approximately similar concentrations (nanomolar range) of both EII-AF488 and EII-AF633 were mixed in either a decylPEG or $C_{10}E_5$ buffer system in the absence or the presence of 1 mM mannitol. The cloud-points for decylPEG and $C_{10}E_5$ are 58° and 41°C, respectively. The mixtures were placed for 20 min at either room temperature (RT; ~18°C) or 30°C. Such an increase in temperature is expected to increase the rate of subunit exchange (Broos et al. 1998). After the incubation period, the fractions were placed on ice to stop the exchange and analyzed with FCCS. The FCCS measurements, carried out at RT, lasted only 2–3 min, and this period is not expected to significantly alter the amount of subunit exchange. In Figure 3A, the autocorrelation curves are shown for AF488- and AF633-labeled EII-R636C in $C_{10}E_5$, incubated at 30°C in the presence of mannitol (a schematic of the subunit exchange between homodimers is shown in Fig. 3B). The fit quality of the curves with a one-species model was good (see residuals) and did not improve significantly when a two-species model was used (not shown). For EII-AF488 and EII-AF633, diffusion constants were calculated of 34.5 ± 2.5 μm^2/sec and 37.0 ± 2.0 μm^2/sec, respectively. The results of the various experiments are summarized in Figure 3C. When EII-AF488 and EII-AF633 were mixed in a decylPEG buffer system (in the absence of mannitol) at either RT or 30°C, no significant subunit exchange was observed. However, as expected, a lower cloud-point or a higher incubation temperature promoted the subunit exchange between EII-AF488 and EII-AF633. These results exemplify the stimulating effect of a lower cloud-point or a higher incubation temperature on the subunit exchange of EII. We did not observe a difference in the diffusion constant for labeled EII-R636C in either decylPEG or $C_{10}E_5$ (data not shown). Also, for mannitol-bound EII-R636C, we did not observe a different diffusion constant compared with the diffusion constant in the absence of mannitol. Importantly, the

Table 1. *Parameters obtained from the double-labeled DNA oligomers*

Parameter	Green (λ_{ex} = 488 nm)	Red (λ_{ex} = 633 nm)	Cross-correlation
τ_{dif} (μsec)	100	150	155
N	4.8	16.2	15.0
D (μm^2/sec)	81	96	—
C ($1/\mu m^3$)	24	35	—

(τ_{dif}) Diffusion time, (N) effective particle number, (D) diffusion constant, (C) concentration.

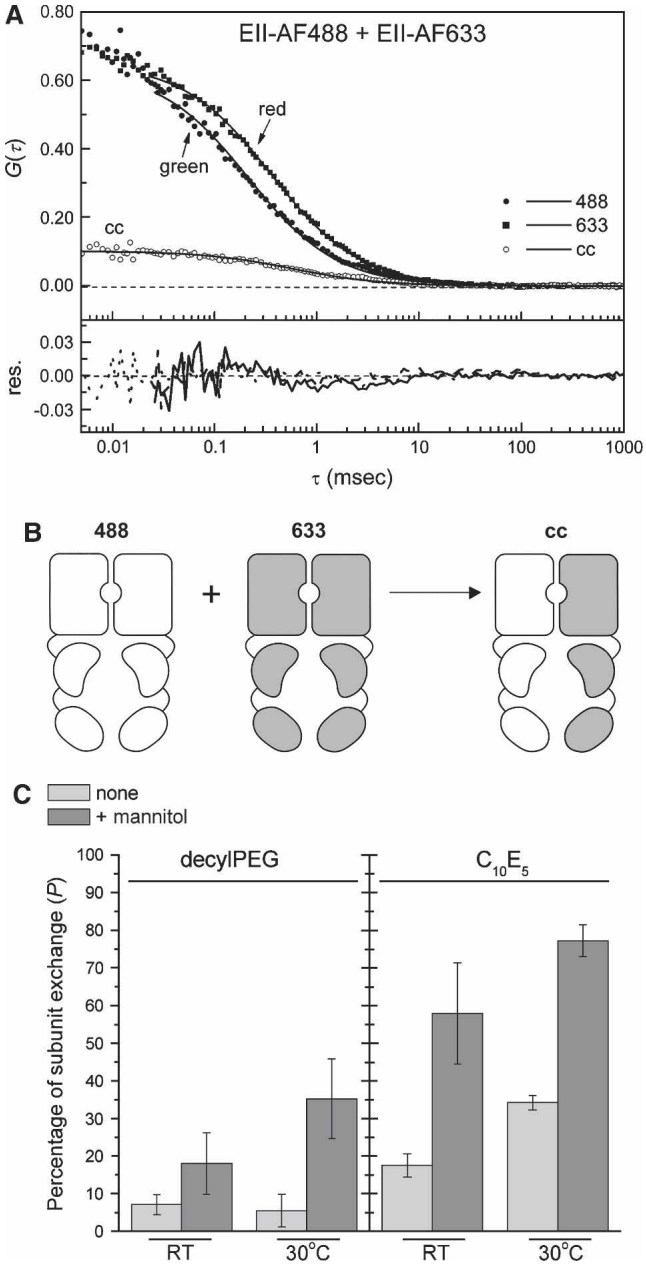

Figure 3. Effect of the buffer system on the subunit exchange between EII-AF488 and EII-AF633 homodimers. (*A*) Autocorrelation curves of mixed EII-AF488 and EII-AF633 and the cross-correlation curve. The protein samples (nanomolar concentrations) were prepared in a $C_{10}E_5$-containing buffer supplemented with 1 mM mannitol and incubated for 20 min at 30°C, after which the FCCS measurements were started. The quality of the one-species 3D-diffusion model toward which the data were fitted is shown by the residuals. (*B*) Schematic of the subunit exchange between homodimers 488 and 633, resulting in heterodimer cross-correlation. (*C*) Mixtures of 25 nM EII-AF488 and EII-AF633 were prepared in either a decylPEG or $C_{10}E_5$-containing buffer, in the absence (light gray) or presence (dark gray) of 1 mM mannitol and incubated for 20 min at either RT or 30°C, after which the FCCS measurements were started. The maximal amount of cross-correlation was calculated as described in Materials and Methods. The error bars represent the standard deviation of three to six individual measurements.

addition of mannitol, prior to homodimer mixing, enhanced the subunit exchange.

Subunit exchange at different stages of the catalytic cycle

The subunit exchange in the $C_{10}E_5$-buffer system was investigated further in a time-dependent manner under conditions of substrate binding and protein phosphorylation. The effect of substrate binding on the subunit exchange kinetics is shown in Figure 4. Without mannitol (open circles), the exchange was slow and reached ~60% after ~40 min. The presence of mannitol (solid circles) enhanced the exchange rate about fourfold. Clearly, the increase in subunit exchange suggests that mannitol binding induces an increase in the dissociation rate constant of the associated complex or a decrease in the association rate constant of the individual subunit, or both. An opposite effect on the subunit exchange kinetics was observed when the EII samples were phosphorylated prior to homodimer mixing. Mixtures of EII-AF488 and EII-AF633 were separately prephosphorylated for 10 min at 30°C (see Materials and Methods), after which they were mixed and incubated for up to 40 min at 30°C to allow subunit exchange. Phosphorylation of the proteins significantly decreased the exchange rate (Fig. 4, squares). After 40 min of incubation, only ~20% of the maximum amount of exchange was reached (compared with the mannitol-treated samples). There was no effect of the individual components of the phosphorylation assay (e.g., EI, HPr, PEP, $MgCl_2$) on the rate of subunit exchange (not shown).

Next, we analyzed the effect of substrate binding and phosphorylation of EII^{mtl} on the exchange kinetics of the enzyme. Since mannitol binding to the phosphorylated enzyme results in immediate phosphoryl transfer to the substrate and subsequent release of mannitol-1-P, we used perseitol rather than mannitol as a substrate analog. Perseitol is a linear alditol with an additional C atom compared with mannitol and binds to EII^{mtl} with relative high affinity (K_D = ~800 nM), but this molecule cannot become phosphorylated by EII^{mtl} (Lolkema et al. 1993b). Experiments were carried out with the unphosphorylated and phosphorylated species in either the absence or the presence of 1 mM perseitol. The unphosphorylated homodimers, preincubated with perseitol, showed after mixing essentially the same subunit exchange kinetics as when mannitol was used (not shown). However, addition of perseitol to prephosphorylated homodimers significantly increased the exchange rate (Fig. 4, stars) when compared with that of the phosphorylated species without substrate (Fig. 4, solid squares). This suggests that binding of perseitol (and likely mannitol) to EII^{mtl} counteracts the decreased exchange observed for the phosphorylated species.

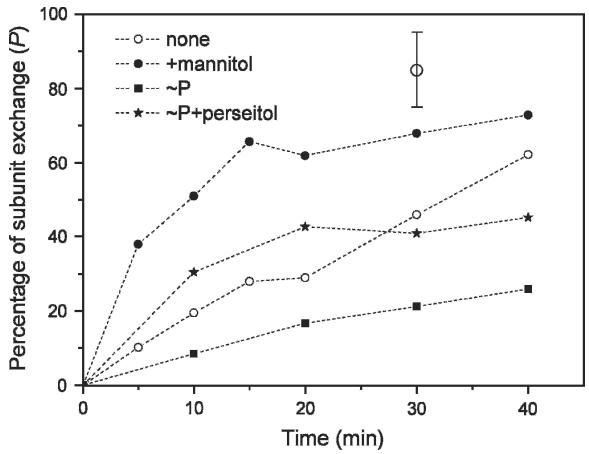

Figure 4. Time dependence of subunit exchange at different steps of the catalytic cycle. Mixtures of 25 nM EII-AF488 and EII-AF633 were prepared in a $C_{10}E_5$-containing buffer and placed for up to 40 min at 30°C in the absence (open circles) or the presence (solid circles) of 1 mM mannitol. To prephosphorylate the separate samples of EII-AF488 and EII-AF633, the phosphorylation components (see Materials and Methods) were added and the samples were placed for 10 min at 30°C to allow complete phosphorylation of EII^{mtl}, after which the samples were mixed and placed for up to 40 min at 30°C (squares). Addition of 1 mM perseitol was performed right after the mixing of the prephosphorylated samples (stars). The amount maximal amount of cross-correlation was calculated as described in Materials and Methods. The error bar reflects the typical error of three to six individual measurements.

Discussion

In this paper we have addressed the oligomeric state and stability of EII^{mtl} at different states of the catalytic cycle, that is, the unphosphorylated and the phosphorylated forms, either in the substrate-free or substrate-bound configuration. The main findings are that (1) detergent-solubilized EII^{mtl} forms very stable dimers (at nanomolar concentrations) with an apparent subunit exchange rate constant of $\sim 3.5 \times 10^{-4}$ sec^{-1}; (2) mannitol binding increases this rate constant about four times, whereas (3) phosphorylation decreases the rate constant about four times. Furthermore, binding of substrate to the phosphorylated protein antagonizes the stabilizing effect of protein phosphorylation. A schematic representation of these three conformational states is shown in Figure 5.

The oligomeric state of EII^{mtl}

From a range of studies, it has been concluded that EII^{mtl} forms an oligomeric species, most likely dimeric, both in the native membrane and in the detergent-solubilized state. On the basis of the count rate per particle obtained from the autocorrelation curves of both the labeled EII^{mtl} species and the free dyes, the majority of EII^{mtl} was in a dimeric state. For the Alexa Fluor–labeled DNA oligomers, we observed count rates per particle for the green and the red channels of 3.6 and 3.9 kHz, respectively. For the Alexa Fluor–labeled EII^{mtl} preparations, count rates per particle were 6.7 and 8.7 kHz, respectively (measured with samples at time point t = 0 min in Fig. 4). The doubling of the count rate for EII^{mtl} as compared with single-labeled DNA shows that most of the EII^{mtl} is in a dimeric state. Furthermore, the total number of particles observed in the observation volumes (for both the green and the red detector) proved to be constant during the experiments (not shown), indicating that essentially all of the EII^{mtl} species remained dimeric after substrate binding and/or phosphorylation. However, for a subunit exchange reaction to occur, monomeric particles must be present at any given time. Given the timescale of subunit exchange (up to hours for the phosphorylated species), and the observation that >95% of EII^{mtl} is in a dimeric state, we propose that the EII^{mtl} monomers are only transiently formed. EII^{mtl} presumably has a very high association rate constant and a very low dissociation rate constant, giving rise to the low K_D of the monomer–dimer equilibrium. Mannitol binding to and/or phosphorylation of EII^{mtl} seem to affect the rate constants of association and dissociation, but the equilibrium binding constant is such that the enzyme remains predominantly dimeric at the enzyme concentrations investigated (the lowest concentration of EII^{mtl} was ~1 nM).

These findings are important for the interpretation of the data presented in Figure 4. Since EII-AF488 and EII-AF633 were mixed approximately in a 1:1 ratio, the maximal fraction of EII-AF488/EII-AF633 heterocomplexes is 0.5 (assuming random association of the different species). For the analysis of the cross-correlation data, the fraction of 0.5 was set to 100% (and corrected for the small spatial misalignment of the green and the red observation volumes). The observation that ultimately >80% subunit exchange was reached (Figs. 3C, 4) indicates that most of the EII^{mtl} is in a functional state.

Comparison with other data

The observation of an increase in subunit exchange upon binding of mannitol is in line with earlier work; that is, the recovery of activity upon mixing of two inactive mutants (IIC^{mtl} and EII^{mtl}-G196D) was found to proceed

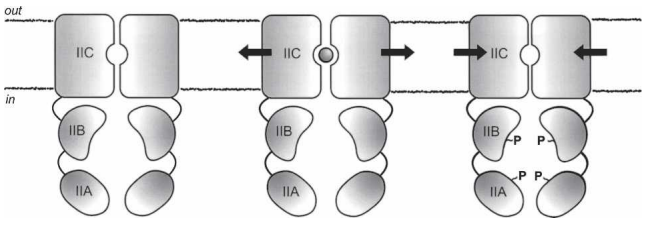

Figure 5. Schematic of the oligomeric stability of EII^{mtl} at different stages of the catalytic cycle. The arrows indicate the force applied on the dimeric state due to substrate binding (circle between the domains) or protein phosphorylation (~P).

faster when the mixture was preincubated with mannitol (Broos et al. 1998). In analogy with these observations and the observations in this study, mannitol has been suggested to dissociate EII^{mtl} (Stephan and Jacobson 1986). By examining HPr-dependent phosphorylation kinetics, it was concluded that phosphorylated EII^{mtl} is more stable (associates more easily) than the unphosphorylated enzyme (Roossien et al. 1984; Robillard and Blaauw 1987). These findings have been confirmed with the experiments described in this article and further suggest that considering the strength of the dimer, conformational changes occur upon binding of mannitol and phosphorylation that alter the stability of the enzyme. Calorimetry data have indicated that binding of mannitol leads to an effective water shielding of 50–60 residues as a consequence of a change in the IIC^{mtl}/IIB^{mtl} domain interaction (Meijberg et al. 1998). Residue 134 has been shown to be located at the dimer interface, as was inferred from its ability to form an intersubunit disulfide when mutated into a cysteine (Van Montfort et al. 2002). Interestingly, upon binding of mannitol, cross-linking of Cys134 was no longer observed, suggesting that at least this part of the structure changes its conformation and moves apart. In line with large structural alterations in EII^{mtl} upon substrate binding are the observations of a structuring effect in the region of residues 125–150 upon binding of mannitol, whereas the environment around residue 97 (proposed to be in a β-sheet configuration) becomes largely unfolded (Veldhuis et al. 2005b). The latter residue is located near the mannitol-binding site, as was judged from a large decrease in Trp fluorescence of single Trp, EII-F97W, upon binding of azimannitol, a mannitol analog that is a Trp-fluorescence resonance energy transfer acceptor (E.P.P. Vos, in prep.).

There is now compelling evidence that EII^{mtl} has a single mannitol-binding site per dimer (Veldhuis et al. 2005a). It also has been shown that mannitol is bound near the first transmembrane helix and that this helix is located at the dimer interface (Van Montfort et al. 2001; Broos et al. 2002). This suggests that mannitol is bound at the dimer interface in between the two IIC^{mtl}-subunits. Together with large structural rearrangements in the IIC^{mtl}-domain around the dimer interface upon binding of mannitol (Broos et al. 2000; Veldhuis et al. 2005b; this study), this part of the structure of EII^{mtl} seems directly involved in the communication between the two subunits. Currently, the information is limited in respect to the residues that are located at the dimer interface and are responsible for the high association of the two IIC^{mtl}-subunits. The methodology presented in this paper allows the screening of EII^{mtl}-mutants hampered in the association.

In conclusion, FCCS enabled us to monitor the kinetics of subunit exchange in the dimeric mannitol transporter, EII^{mtl}, from *E. coli*. The data suggest that upon binding of mannitol, the dimeric structure is loosened, which may be critical for the phosphorylated IIB^{mtl}-domain to interact with the membrane-embedded IIC^{mtl}-domain and transfer of the phosphoryl group to mannitol. Upon phosphorylation of $IIBA^{mtl}$ and in the absence of mannitol, EII^{mtl} becomes tighter, and this may reflect additional IIC^{mtl}–IIC^{mtl} interdomain interactions (e.g., as observed in previous calorimetry experiments; Meijberg et al. 1998). An intermediate situation is observed in the catalytically competent state, that is, both when substrate is present and the enzyme is phosphorylated. Apparently, the destabilizing effect of substrate binding is antagonized by additional domain–domain interactions as a consequence of phosphorylation of the IIB^{mtl}-domain.

Materials and methods

Chemicals and reagents

D-[1-^{3}H(N)]Mannitol (17.0 Ci/mmol, batch no. 3499–326) was purchased from NEN Research Products. D-[1-^{14}C]Mannitol (59.0 mCi/mmol, batch no. 78) was purchased from Amersham Biosciences. Radioactivity measurements were performed using Emulsifier Scintillator Plus, obtained from Packard. Q-Sepharose Fast Flow and Ni-NTA resin were from Amersham Biosciences. L-Histidine, imidazole, and N-ethylmaleimide (NEM) were from Fluka. Alexa fluorophores with a maleimide reactive group were purchased from Invitrogen. Alexa Fluor–labeled oligonucleotides were purchased from IBA Nucleic Acid Synthesis (IBA GmbH). Decylpoly(ethylene glycol) 300 (decylPEG) was obtained from Kwant High Vacuum Oil Recycling and Synthesis. The detergent $C_{10}E_5$ (decyl pentaethylene glycol ether) was synthesized and purified as described (Swaving-Dijkstra et al. 1996). His-tagged versions of EI and HPr were created, using standard genetic tools (as will be described elsewhere). All other chemicals used were analytical grade.

Construction of the double-cysteine mutant

Plasmid pMamtlaP_r6HisEII-SSCS (single-cysteine mutant with an N-terminal 6 His-tag) (Van Montfort et al. 2001) was used as a basis. Site-directed mutagenesis with the Stratagene QuikChange mutagenesis kit was employed to mutate Arg636 at the C terminus of the IIA^{mtl}-domain into a cysteine residue, which, together with a silent mutation, resulted in an additional restriction enzyme recognition site (EaeI). The correct sequence was confirmed by nucleotide sequence analysis.

Cell growth, isolation of ISO membrane vesicles, and purification

The plasmids harboring the mutated *mtlA* genes were transformed and subsequently grown in *E. coli* LGS322 [*F^- thi-1, hisG1, argG6, metB1, tonA2, supE44, rspL104, lacY1, galT6, gatR49, gatA50, Δ(mtlA′p), $mtlD^c$, Δ(gutR′MDBA-recA)*] as described (Grisafi et al. 1989; Boer et al. 1994). ISO membrane vesicles with overexpressed levels of EII^{mtl} were prepared by passage of cells through a French Press at 10,000 psi, essentially as described (Broos et al. 1999). The membrane vesicles were washed once in 25 mM Tris-HCl (pH 7.6), 5 mM DTT, and

1 mM NaN_3, and quickly frozen in small aliquots in liquid nitrogen prior to storage at −80°C. For mannitol binding experiments or purification of EII^{mtl}, membrane vesicles were placed at 37°C for quick thawing and thereafter directly placed on ice until further use. Extraction of EII^{mtl} from the membrane vesicles and purification using Ni-NTA affinity chromatography were performed as described (Veldhuis et al. 2005a). Further purification procedures for the Alexa Fluor–labeled mutants are described below.

Mannitol-binding experiments and phosphorylation activity measurements

Mannitol-binding experiments were used to estimate the affinity of EII^{mtl} for mannitol and the number of binding sites (Veldhuis et al. 2004), assuming one binding site per two subunits of EII^{mtl} (Veldhuis et al. 2005a). The nonvectorial PEP-dependent phosphorylation activity, catalyzed by EII^{mtl}, was measured as described (Robillard and Blaauw 1987). Briefly, the assay mixture contained 25 mM Tris-HCl (pH 7.6), 5 mM DTT, 5 mM $MgCl_2$, 5 mM PEP, 350 nM EI, 17 μM HPr, with or without 0.25% decylPEG/$C_{10}E_5$, and rate-limiting amounts of EII^{mtl} (nanomolar range). After incubation of the mixture for 5 min at 30°C, the reaction was started by adding 1 mM ^{14}C-mannitol. The reaction was quenched at given time intervals by loading the samples on Dowex AG1-X2 columns. After washing the column with four column volumes of H_2O, formed ^{14}C-mannitol-1-P was eluted using two column volumes of 0.2 N HCl and quantified by liquid scintillation counting. Specific phosphorylation activities are given in min^{-1} (nM mannitol-1-P formed per minute per nM EII^{mtl}).

Phospho-protection of Cys384 and alkylation of Cys636

To site-specifically label the engineered cysteine at position 636, and not the catalytically important cysteine at position 384, Cys384 was protected from alkylation by maleimides by phosphorylation of the thiol using the native phosphorylation cascade. First, EII^{mtl} and EI were fully reduced. Therefore, mixtures of 750 μL of purified EII-R636C (final concentration of 3–7 μM) were prepared in 25 mM NaP_i (pH 7.4), 20 mM EDTA, 5 mM freshly prepared DTT, 0.25% decylPEG, and 50 nM EI. The mixtures were incubated for 5 min at RT and subsequently desalted using a NAP-10 desalting column (Amersham Biosciences). Next, 5 mM PEP, 5 mM $MgCl_2$ and 11.5 μM HPr were added, and the mixture was placed for 15 min at 30°C, ensuring phosphorylation of all Cys384 residues. The addition of 100–200 nmol (25–50 equivalents) of alkylating reagent (Alexa Fluor 488/633 or NEM) was followed by a labeling reaction for 30 min at 30°C, after which the reaction was quenched by addition of 10 mM β-mercaptoethanol. Excess of unreacted label was removed by another desalting step using a NAP-10 column. In the case of labeling with Alexa 488, the mixture was further purified by Q-Sepharose affinity column chromatography as described (Veldhuis et al. 2005a). Alexa 633 has a very strong affinity for Q-Sepharose (not shown) and was further purified by Ni-NTA chromatography (Veldhuis et al. 2005a), followed by desalting on a Micro Bio-Spin column (Bio-Rad). In all cases, the final buffer composition was 25 mM Tris-HCl (pH 7.6), 400 mM NaCl, 10 mM β-mercaptoethanol, supplemented with detergent as specified in the text. The stoichiometry of labeling was estimated from light absorption measurements. To correct for the absorption of the Alexa dyes in the UV region, the spectra of the free labels were used. Subtraction of the spectra of free label from the spectra of labeled protein resulted in characteristic Trp/Tyr-protein absorption spectra, allowing for the estimation of the protein concentration, and thereby the stoichiometry of labeling. The calculated extinction coefficient for EII-R636C was 31,190 $L \cdot mol^{-1} \cdot cm^{-1}$ (Pace et al. 1995).

Fluorescence cross-correlation spectroscopy

FCCS measurements were carried out on a dual-color laser scanning confocal microscope (LSCM). The LSCM is based on an inverted Axiovert S 100 TV microscope (Zeiss) in combination with a galvanometer optical scanner (model 6860, Cambridge Technology) and a microscope objective nanofocusing device (P-721, PI). The two laser beams (488 nm, argon ion laser, Spectra-Physics; 633 nm, He-Ne laser, JDS Uniphase) were focused by a Zeiss C-Apochromat infinity-corrected 1.2 NA 63× water-immersion objective for excitation of the Alexa Fluor 488 and 633 fluorophores. The fluorescence was collected through the same objective, separated from the excitation beams by a beam pick-off plate (BSP20-A1, ThorLabs), split into two channels by a dichroic beam splitter (585DCXR, Chroma Technology), and finally directed through emission filters (HQ 535/50 and HQ 675/50, Chroma Technology) and pinholes (diameter of 30 μm) onto two avalanche photodiodes (SPCM-AQR-14, EG&G). The fluorescence signals were digitized, and auto- and cross-correlation curves were calculated on a PC using a multiple τ algorithm. The setup was calibrated by measuring the known diffusion coefficients of Alexa Fluor 488 and 633 in water at 20°C (Invitrogen) ($D = 300\ \mu m^2/sec$). The detection volumes for 488 and 633 nm excitation were ~0.20 fL and ~0.45 fL, respectively, with $1/e^2$ lateral radii of 180 and 240 nm, respectively. Cross-correlation measurements of a double-labeled (Alexa Fluor 488 and 633), double-stranded oligonucleotide were used to align and maximize the overlap between the two observation volumes. For this, the oligonucleotides 5′-AF488-ATTATTGAGTGGTCACTTTAAA-3′ and 5′-AF633-TTTAAAG TGACCACTCAATAAT-3′ were boiled together for 5 min at a final concentration of ~40 nM and subsequently slowly cooled to 4°C to allow annealing. Afterward, 1 mM NaN_3 was added as a preservative. In the experiments, the amount of cross-talk was evaluated and found to be negligible. Autocorrelation curves were fitted with a one-component, three-dimensional diffusion model (Aragón and Pecora 1976), using Origin software (OriginLab).

The concentrations of 488-labeled (*g,g*), 633-labeled (*r,r*), and 488/633-labeled particles (*g,r*) within the observation volumes were calculated on the assumption that only dimeric enzyme II species were present. The autocorrelation function $G(\tau)$ and the diffusion time τ_{dif} for three-dimensional Brownian diffusion of *S* species with identical diffusion constants *D*, but different values for the molecular brightness *Q* (product of the absorption cross sections and the fluorescence quantum yields) and concentrations *C,* are given by

$$G(\tau) = \frac{\sum_{i \in S} Q_i^2 C_i}{V_{eff} \left(\sum_{i \in S} Q_i C_i \right)^2} \left(1 + \frac{\tau}{\tau_{dif}} \right)^{-1} \left(1 + \frac{\tau}{f^2 \tau_{dif}} \right)^{-1/2} \text{with} \quad (1)$$

$$\tau_{dif} = \frac{\omega^2}{4D} \text{ (Aragón and Pecora 1976)} \quad (2)$$

where ω and z are the effective radii in the lateral and axial direction of the observation volume V_{eff}, and f ($=z/\omega$) is the structure parameter (Rigler et al. 1993). In the case in which there are both heterodimers with two different fluorescent labels (g,r) and homodimers with two identical fluorescent labels (g,g and r,r) present, the amplitudes of the individual autocorrelation curves are given by

$$G_g(0) = \frac{C_{g,r} + Q^2 C_{g,g}}{V_g\left(C_{g,r} + QC_{g,g}\right)^2} \quad (3)$$

$$G_r(0) = \frac{C_{g,r} + Q^2 C_{r,r}}{V_r\left(C_{g,r} + QC_{r,r}\right)^2} \quad (4)$$

with $Q = 2$, if it is assumed that homodimers have twice the quantum yield as heterodimers. $C_{g,r}$ corresponds to the concentration of heterodimers; $C_{g,g}$ and $C_{r,r}$ correspond to the concentrations of the homodimers. V_g and V_r are the effective observation volumes of the blue and the red channels and are defined as

$$V_i = \pi^{3/2}\omega_i^3 f_i \quad (5)$$

For the cross-correlation curve, the amplitude is (Schwille et al. 1997)

$$G_{g,r}(0) = \frac{C_{g,r}}{V_{g,r}\left(C_{g,r} + 2C_{g,g}\right)\left(C_{g,r} + 2C_{r,r}\right)} \quad (6)$$

with $V_{g,r}$ being the effective cross-correlation observation volume that can be derived from Equation 5 using

$$\omega_{g,r} = \sqrt{\frac{\omega_r^2 + \omega_g^2}{2}} \quad (7)$$

$$z_{g,r} = \sqrt{\frac{z_r^2 + z_g^2}{2}} \quad (8)$$

The fraction (F) of heterodimers to total dimers is defined as:

$$F = \frac{C_{g,r}}{C_{g,g} + C_{r,r} + C_{g,r}} \quad (9)$$

In the case of full subunit exchange and a binomial distribution, the maximum fraction of heterodimers (F_{bin}) that can be reached with a starting solution with concentrations $C_{g,g}$, $C_{r,r}$, and $C_{g,r}$, is:

$$F_{\text{bin}} = \frac{\left(2C_{g,g} + C_{g,r}\right)\left(2C_{r,r} + C_{g,r}\right)}{2\left(C_{g,g} + C_{r,r} + C_{g,r}\right)^2} \quad (10)$$

Based on the measured $G_g(0)$, $G_r(0)$, and $G_{gr}(0)$ concentrations $C_{g,g}$, $C_{r,r}$, and $C_{g,r}$ were calculated for each measurement by solving Equations 3–6. In turn, F and F_{bin} were calculated using Equations 9and 10. Finally, the percentage P of subunit exchange between the dimers relative to the maximum exchange F_{bin} was calculated by:

$$P = \frac{F}{F_{\text{bin}}} \times 100\ \% \quad (11)$$

Acknowledgments

This work was supported by the Netherlands Foundation for Chemical Research (CW) with financial aid from the Netherlands Organization for the Advancement of Scientific Research and the Materials Science Centre^{plus}.

References

Ambudkar, S.V., Anantharam, V., and Maloney, P.C. 1990. UhpT, the sugar phosphate antiporter of *Escherichia coli*, functions as a monomer. *J. Biol. Chem.* **265:** 12287–12292.

Aragón, S.R. and Pecora, R. 1976. Fluorescence correlation spectroscopy as a probe of molecular dynamics. *J. Chem. Phys.* **64:** 1791–1803.

Boer, H., Ten Hoeve-Duurkens, R.H., Schuurman-Wolters, G.K., Dijkstra, A., and Robillard, G.T. 1994. Expression, purification and kinetic characterization of the mannitol transport domain of the phosphoenolpyruvate-dependent mannitol phosphotransferase system of *Escherichia coli*. *J. Biol. Chem.* **269:** 17863–17871.

Boer, H., Ten Hoeve-Duurkens, R.H., and Robillard, G.T. 1996. Relation between the oligomerization state and the transport and phosphorylation function of the *Escherichia coli* mannitol transport protein: Interaction between mannitol-specific enzyme II monomers studied by complementation of inactive site-directed mutants. *Biochemistry* **35:** 12901–12908.

Briggs, C.E., Khandekar, S.S., and Jacobson, G.R. 1992. Structure/function relationships in the *Escherichia coli* mannitol permease: Identification of regions important for membrane insertion, substrate binding and oligomerization. *Res. Microbiol.* **143:** 139–149.

Broos, J., Ten Hoeve-Duurkens, R.H., and Robillard, G.T. 1998. A mechanism to alter reversibly the oligomeric state of a membrane-bound protein demonstrated with *Escherichia coli* EIImtl in solution. *J. Biol. Chem.* **273:** 3865–3870.

Broos, J., Ter Veld, F., and Robillard, G.T. 1999. Membrane protein–ligand interactions in *Escherichia coli* vesicles and living cells monitored via a biosynthetically incorporated tryptophan analogue. *Biochemistry* **38:** 9798–9803.

Broos, J., Strambini, G.B., Gonnelli, M., Vos, E.P.P., Koolhof, M., and Robillard, G.T. 2000. Sensitive monitoring of the dynamics of a membrane-bound transport protein by tryptophan phosphorescence spectroscopy. *Biochemistry* **39:** 10877–10883.

Broos, J., Pas, H.H., and Robillard, G.T. 2002. The smallest resonance energy transfer acceptor for tryptophan. *J. Am. Chem. Soc.* **124:** 6812–6813.

Casey, J.R. and Reithmeier, R.A.F. 1991. Analysis of the oligomeric state of Band 3, the anion transport protein of the human erythrocyte membrane, by size exclusion high performance liquid chromatography. Oligomeric stability and origin of heterogeneity. *J. Biol. Chem.* **266:** 15726–15737.

Eigen, M. and Rigler, R. 1994. Sorting single molecules. Applications to diagnostics and evolutionary biotechnology. *Proc. Natl. Acad. Sci.* **91:** 5740–5747.

Friesen, R.H., Knol, J., and Poolman, B. 2000. Quaternary structure of the lactose transport protein of *Streptococcus thermophilus* in the detergent-solubilized and membrane-reconstituted state. *J. Biol. Chem.* **275:** 33527–33535.

Geertsma, E.R., Duurkens, R.H., and Poolman, B. 2005. Functional interactions between subunits of the lactose transporter from *Streptococcus thermophilus*. *J. Mol. Biol.* **350:** 102–111.

Gerchman, Y., Rimon, A., Venturi, M., and Padan, E. 2001. Oligomerization of NhaA, the Na^+/H^+-antiporter of *Escherichia coli* in the membrane and its functional and structural consequences. *Biochemistry* **40:** 3403–3412.

Gösch, M. and Rigler, R. 2005. Fluorescence correlation spectroscopy of molecular motions and kinetics. *Adv. Drug Deliv. Rev.* **57:** 169–190.

Grisafi, P.L., Scholle, A., Sugiyama, J., Briggs, C., Jacobson, G.R., and Lengeler, J.W. 1989. Deletion mutants of the *Escherichia coli* K-12 mannitol permease: Dissection of transport-phosphorylation, phospho-exchange, and mannitol-binding activities. *J. Bacteriol.* **171:** 2719–2727.

Haustein, E. and Schwille, P. 2003. Ultrasensitive investigations of biological systems by fluorescence correlation spectroscopy. *Methods* **29:** 153–166.

———. 2004. Single-molecule spectroscopic methods. *Curr. Opin. Struct. Biol.* **14:** 531–540.

Hebert, D.N. and Carruthers, A. 1992. Glucose transporter oligomeric structure determines transporter function. Reversible redox-dependent interconversions of tetrameric and dimeric GLUT1. *J. Biol. Chem.* **267:** 23829–23838.

Hink, M. 2002. ''Fluorescence correlation spectroscopy applied to living plant cells.'' Ph.D. thesis, Wageningen University, Wageningen, The Netherlands.

Khandekar, S.S. and Jacobson, G.R. 1989. Evidence for two distinct conformations of the *Escherichia coli* mannitol permease that are important for its transport and phosphorylation functions. *J. Cell. Biochem.* **39:** 207–216.

Leonard, J.E. and Saier Jr., M.H. 1983. Mannitol-specific enzyme II of the bacterial phosphotransferase system. II. Reconstitution of vectorial transphosphorylation in phospholipid vesicles. *J. Biol. Chem.* **258:** 10757–10760.

Lolkema, J.S. and Robillard, G.T. 1990. Subunit structure and activity of the mannitol-specific Enzyme II of the *Escherichia coli* phosphoenolpyruvate-dependent phosphotransferase system solubilized in detergent. *Biochemistry* **29:** 10120–10125.

Lolkema, J.S., Kuiper, H., Ten Hoeve-Duurkens, R.H., and Robillard, G.T. 1993a. Mannitol-specific Enzyme II of the phosphoenolpyruvate-dependent phosphotransferase system of *Escherichia coli*: Physical size of Enzyme II^{mtl} and its domain IIBA and IIC in the active state. *Biochemistry* **32:** 1396–1400.

Lolkema, J.S., Wartna, E.S., and Robillard, G.T. 1993b. Binding of the substrate analogue perseitol to phosphorylated and unphosphorylated Enzyme II^{mtl} of the phosphoenolpyruvate-dependent phosphotransferase system of *Escherichia coli*. *Biochemistry* **32:** 5848–5854.

Meijberg, W., Schuurman-Wolters, G.K., and Robillard, G.T. 1998. Thermodynamic evidence for conformational coupling between the B and C domains of the mannitol transporter of *Escherichia coli*, Enzyme II^{mtl}. *J. Biol. Chem.* **273:** 7949–7956.

Meseth, U., Wohland, T., Rigler, R., and Vogel, H. 1999. Resolution of fluorescence correlation measurements. *Biophys. J.* **76:** 1619–1631.

Pace, C.N., Vajdos, F., Fee, L., Grimsley, G., and Gray, T. 1995. How to measure and predict the molar absorption coefficient of a protein. *Protein Sci.* **4:** 2411–2423.

Pas, H.H., Ellory, J.C., and Robillard, G.T. 1987. Bacterial phosphoenolpyruvate-dependent phosphotransferase system: Association state of membrane-bound mannitol-specific enzyme II demonstrated by inactivation. *Biochemistry* **26:** 6689–6696.

Rigler, R., Mets, Ü., Widengren, J., and Kask, P. 1993. Fluorescence correlation spectroscopy with high count rate and low background: Analysis of translational diffusion. *Eur. Biophys. J.* **22:** 169–175.

Robillard, G.T. and Blaauw, M. 1987. Enzyme II of the *Escherichia coli* phosphoenolpyruvate-dependent phosphotransferase system: Protein–protein and protein–phospholipid interactions. *Biochemistry* **26:** 5796–5803.

Robillard, G.T. and Broos, J. 1999. Structure/function studies on the bacterial carbohydrate transporters, enzyme II, of the phosphoenolpyruvate-dependent phosphotransferase system. *Biochim. Biophys. Acta* **1422:** 73–104.

Roossien, F.F. and Robillard, G.T. 1984. Mannitol-specific carrier protein from the *Escherichia coli* phosphoenolpyruvate-dependent phosphotransferase system can be extracted as a dimer from the membrane. *Biochemistry* **23:** 41–44.

Roossien, F.F., Blaauw, M., and Robillard, G.T. 1984. Kinetics and subunit interaction of the mannitol-specific enzyme II of the *Escherichia coli* phosphoenolpyruvate-dependent phosphotransferase system. *Biochemistry* **23:** 4934–4939.

Roossien, F.F., Van Es-Spiekman, W., and Robillard, G.T. 1986. Dimeric enzyme IImtl of the *E. coli* phosphoenolpyruvate-dependent phosphotransferase system. Cross-linking studies with bifunctional sulfhydryl reagents. *FEBS Lett.* **196:** 284–290.

Sahin-Toth, M., Lawrence, M.C., and Kaback, H.R. 1994. Properties of permease dimer, a fusion protein containing two lactose permease molecules from *Escherichia coli*. *Proc. Natl. Acad. Sci.* **91:** 5421–5425.

Saier Jr., M.H. 1980. Catalytic activities associated with the enzymes II of the bacterial phosphotransferase system. *J. Supramol. Struct.* **14:** 281–294.

Saraceni-Richards, C.A. and Jacobson, G.R. 1997. A conserved glutamate residue, Glu-257, is important for substrate binding and transport by the *Escherichia coli* mannitol permease. *J. Bacteriol.* **179:** 1135–1142.

Schwille, P., Almes-Meyer, F.J., and Rigler, R. 1997. Dual-color fluorescence cross-correlation spectroscopy for multicomponent diffusional analysis in solution. *Biophys. J.* **72:** 1878–1886.

Stephan, M.M. and Jacobson, G.R. 1986. Subunit interactions of the *Escherichia coli* mannitol permease: Correlation with enzyme activities. *Biochemistry* **25:** 4046–4051.

Stephan, M.M., Khandekar, S.S., and Jacobson, G.R. 1989. Hydrophilic C-terminal domain of the *Escherichia coli* mannitol permease: Phosphorylation, functional independence, and evidence for intersubunit phosphotransfer. *Biochemistry* **28:** 7941–7946.

Swaving-Dijkstra, D., Broos, J., and Robillard, G.T. 1996. Membrane proteins and impure detergents: Procedures to purify membrane proteins to a degree suitable for tryptophan fluorescence spectroscopy. *Anal. Biochem.* **240:** 142–147.

Ubarretxena-Belandia, I. and Tate, C.G. 2004. New insights into the structure and oligomeric state of the bacterial multidrug transporter EmrE: An unusual asymmetric homo-dimer. *FEBS Lett.* **564:** 234–238.

Van Montfort, B.A., Schuurman-Wolters, G.K., Duurkens, R.H., Mensen, R., Poolman, B., and Robillard, G.T. 2001. Cysteine cross-linking defines part of the dimer and B/C domain interface of the *Escherichia coli* mannitol permease. *J. Biol. Chem.* **276:** 12756–12763.

Van Montfort, B.A., Schuurman-Wolters, G.K., Wind, J., Broos, J., Robillard, G.T., and Poolman, B. 2002. Mapping of the dimer interface of the *Escherichia coli* mannitol permease by cysteine cross-linking. *J. Biol. Chem.* **277:** 14717–14723.

Van Weeghel, R.P., Meyer, G.H., Keck, W., and Robillard, G.T. 1991a. Phosphoenolpyruvate-dependent mannitol phosphotransferase system of *Escherichia coli*: Overexpression, purification, and characterization of the enzymatically active C-terminal domain of Enzyme IImtl equivalent to Enzyme IIImtl. *Biochemistry* **30:** 1774–1779.

Van Weeghel, R.P., Van der Hoek, Y.Y., Pas, H.H., Elferink, M., Keck, W., and Robillard, G.T. 1991b. Details of mannitol transport in *Escherichia coli* elucidated by site-specific mutagenesis and complementation of phosphorylation site mutants of the phosphoenolpyruvate-dependent mannitol-specific phosphotransferase system. *Biochemistry* **30:** 1768–1773.

Veenhoff, L.M., Heuberger, E.H.M.L., and Poolman, B. 2001. The lactose transport protein is a cooperative dimer with two sugar translocation pathways. *EMBO J.* **20:** 3056–3062.

Veldhuis, G., Vos, E.P.P., Broos, J., Poolman, B., and Scheek, R.M. 2004. Evaluation of the flow-dialysis technique for analysis of protein–ligand interactions: An experimental and a Monte Carlo study. *Biophys. J.* **86:** 1959–1968.

Veldhuis, G., Broos, J., Poolman, B., and Scheek, R.M. 2005a. Stoichiometry and substrate affinity of the mannitol transporter, $EnzymeII^{mtl}$, from *Escherichia coli*. *Biophys. J.* **89:** 201–210.

Veldhuis, G., Gabellieri, E., Vos, E.P.P., Poolman, B., Strambini, G.B., and Broos, J. 2005b. Substrate-induced conformational changes in the membrane-embedded IIC^{mtl}-domain of the mannitol permease from *Escherichia coli,* $EnzymeII^{mtl}$, probed by tryptophan phosphorescence spectroscopy. *J. Biol. Chem.* **280:** 35148–35156.

Weng, Q.-P. and Jacobson, G.R. 1993. Role of a conserved histidine residue, His-195, in the activities of the *Escherichia coli* mannitol permease. *Biochemistry* **32:** 11211–11216.

Weng, Q.-P., Elder, J., and Jacobson, G.R. 1992. Site-specific mutagenesis of residues in the *Escherichia coli* mannitol permease that have been suggested to be important for its phosphorylation and chemoreception functions. *J. Biol. Chem.* **267:** 19529–19535.

White, D.W. and Jacobson, G.R. 1990. Molecular cloning of the C-terminal domain of *Escherichia coli* D-mannitol permease: Expression, phosphorylation, and complementation with C-terminal permease deletion mutants. *J. Bacteriol.* **172:** 1509–1515.

Yin, C.C., Aldema-Ramos, M.L., Borges-Walmsley, M.I., Taylor, R.W., Walmsley, A.R., Levy, S.B., and Bullough, P.A. 2000. The quaternary molecular architecture of TetA, a secondary tetracycline transporter from *Escherichia coli*. *Mol. Microbiol.* **38:** 482–492.

Zulauf, M. 1991. Detergent phenomena in membrane protein crystallization. In *Crystallization of membrane proteins* (ed. H. Michel), pp. 53–72, CRC Press, Boca Raton, FL.